Multi-technique SAR Coseismic Deformation Retrieval and Fault Modeling of the 2025 Mw 7.7 Myanmar Earthquake

Valerio Ruocco[1,2], Silvia Puliero[2], Simone Atzori[2], Cristiano Tolomei[2], Andrea Antonioli[2], Marco Polcari[2], Matteo Albano[2], Marco Moro[2], Salvatore Stramondo[2], Michele Saroli[1,2], Pasquale Striano[3], Fernando Monterroso[3], Manuela Bonano[3], Francesco Casu[3], Claudio De Luca[3], Riccardo Lanari[3].

[1]DICeM - Università degli Studi di Cassino e del Lazio meridionale, Cassino, Italy.
[2]Istituto Nazionale di Geofisica e Vulcanologia, Rome, Italy.
[3]Istituto per il Rilevamento Elettromagnetico dell'Ambiente, Consiglio Nazionale delle Ricerche (IREA-CNR), Naples-Milan, Italy.

Introduction

On 28 March 2025 at 06:20 UTC, a major earthquake of Mw 7.7 occurred in central Myanmar, with its epicenter located along the central segment of the Sagaing Fault, one of the main tectonic structures in Southeast Asia (Bradley & Hubbard, 2025; Vera et al., 2025). The event, characterized by a shallow hypocenter (~10 km), generated intense ground shaking (Modified Mercalli Intensity IX) in densely populated areas, causing significant casualties and widespread infrastructural damage. Effects were felt at distances exceeding 1000 km from the epicentral area, likely related to local seismic amplification controlled by geological conditions (Shahzada et al., 2025). The rupture propagated for approximately 90 s along a ~490 km fault segment, suggesting supershear dynamics, as confirmed by teleseismic data (Vera et al., 2025; Melgar et al., 2025). Twelve minutes after the mainshock, an Mw 6.7 aftershock occurred, likely triggered by static stress changes induced by the main event (USGSa, 2025).

Tectonic Setting

Myanmar is located within a complex tectonic collision zone between the southeastern margin of the Eurasian Plate and the Indian Plate (Mitchell et al., 2012; Tha Zin Htet Tin et al., 2022). The major right-lateral strike-slip Sagaing Fault, extending over 1200 km with a predominantly N–S orientation, accommodates a significant portion of the relative motion between the Burma and Sunda plates, with slip rates estimated at approximately 20 mm/year in the central sections (Vigny et al., 2003; Socquet et al., 2006; Wang et al., 2014; Tha Zin Htet Tin et al., 2022). The area affected by the 2025 earthquake coincides with a known seismic gap identified by previous geological and seismotectonic studies, suggesting long-term elastic strain accumulation and partial rupture of this gap (Hurukawa & Maung Maung, 2011; Bradley & Hubbard, 2025) (Fig.1).

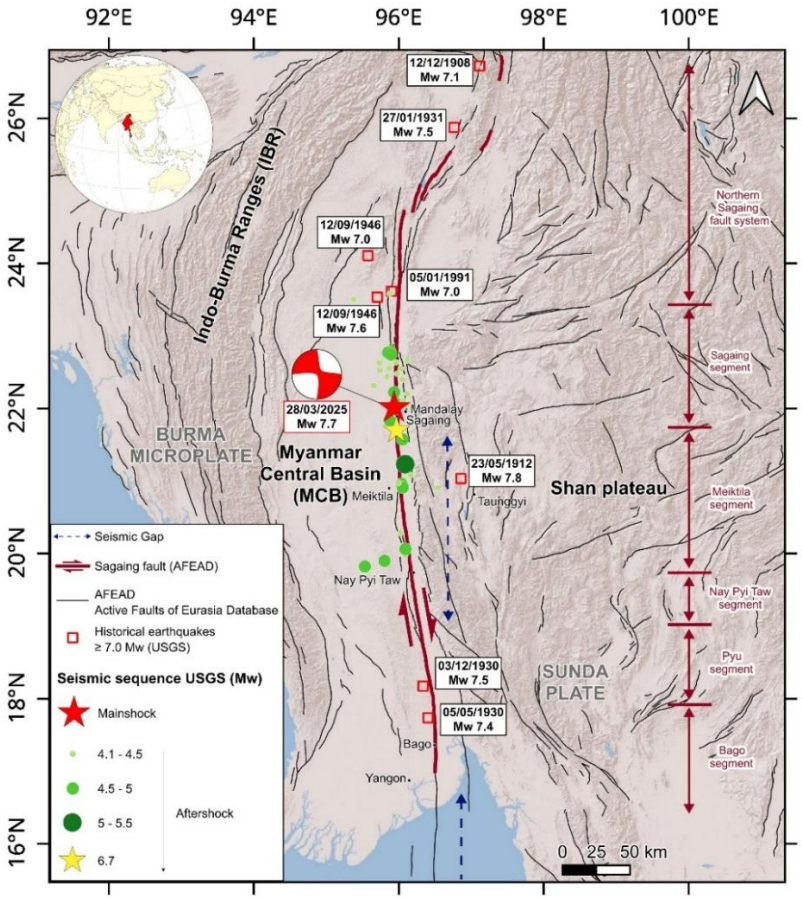

Fig.1 – Overview of the geographical setting and seismicity of the Myanmar area. The focal mechanism of the mainshock is shown together with the aftershocks and the historical earthquakes (USGS, 2025). The active faults are part of the Active Faults of Eurasia Database (AFEAD) (Zelenin et al., 2022). Fault segmentation is based on the classification proposed by Wang et al. (2014). The illustrated seismic gaps refer to the study by Hurukawa and Maung Maung (2011).

Data and Methods

Coseismic deformation associated with the Mw 7.7 event was reconstructed through the integration of SAR Sentinel-1-based techniques: Pixel Offset Tracking (POT) (Gray et al., 1998; Casu et al., 2010, 2011), Multiple Aperture Interferometry (MAI) (Bechor & Zebker, 2006; Jiang et al., 2017), and Interferometric Synthetic Aperture Radar (InSAR) (Massonnet et al., 1993; Massonnet & Feigl, 1998). This integrated approach was crucial to constrain horizontal displacement components, particularly the predominant N–S motion, which is nearly imperceptible with conventional InSAR. Data inversion was conducted in two steps: a nonlinear inversion to estimate the source location, depth, geometry, and rupture mechanism (Okada, 1985; Williams & Wadge, 1998; Atzori et al., 2009), followed by a linear inversion to reconstruct the slip distribution and orientation along the fault (Atzori & Antonioli, 2011; Atzori et al., 2019). A Coulomb Failure Function (ΔCFF) analysis was also performed to assess the interaction between the mainshock and the Mw 6.7 aftershock (Stein et al., 1992; Simpson & Reasemberg, 1994; Harris, 1998).

Results and Discussion

Results show a surface deformation field consistent with right-lateral strike-slip motion along an almost vertical structure, with horizontal displacements reaching ~5 m along the fault trace. Maximum slip occurs in the central segment, corresponding to the seismic gap (Hurukawa & Maung Maung, 2011). The rupture is confined to the upper 15–20 km of the crust and extends for ~490 km,

consistent with supershear propagation (Walker & Shearer, 2009; Petersen et al., 2023; Zeng et al., 2025; Melgar et al., 2025; Vera et al., 2025;) (Fig. 2). Finally, the performed ΔCFF analysis supports the hypothesis that the Mw 6.7 aftershock was triggered by static stress changes (a strong positive static stress transfer, with values up to 1.9 MPa) induced by the mainshock through rupture propagation and stress concentration along the fault system.

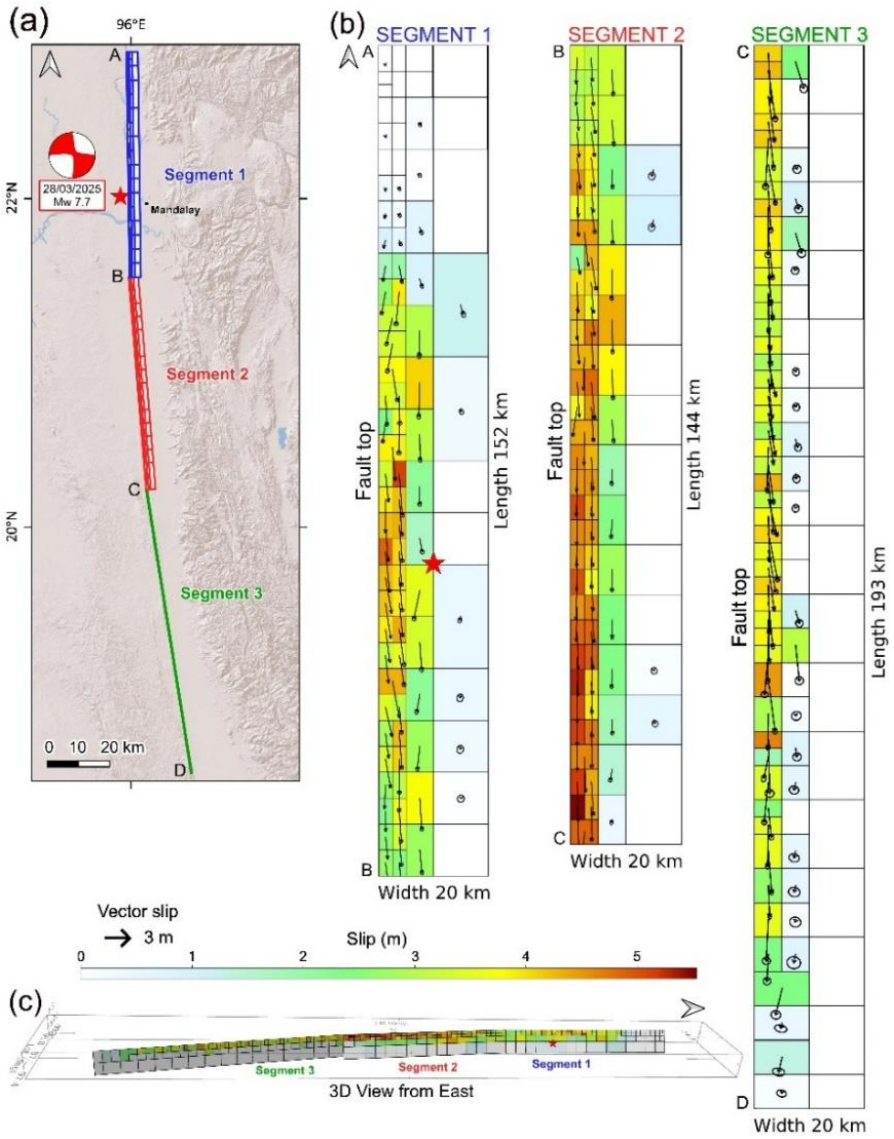

Fig.2 – Modeling of the three segments with the corresponding slip distribution derived from the inversion of InSAR data. (a) The 2D map view; (b) the slip distribution of each segment, in the strike/dip reference system, with associated 1-sigma uncertainties, represented by ellipses for each cell; (c) the 3D view from the east.

Conclusions

The 2025 Mw 7.7 Myanmar earthquake was one of the most significant seismic events in Southeast Asia over the past century. The combined use of different Sentinel-1 datasets enabled full spatial coverage of the rupture extent and a robust characterization of the seismogenic source, including its slip distribution. The results provide new constraints on fault kinematics and segmentation, as well as insights into stress transfer and aftershock triggering mechanisms, with important implications for seismic hazard assessment in the region.

References

Atzori, S., Hunstad, I., Chini, M., Salvi, S., Tolomei, C., Bignami, C., Stramondo, S., Trasatti, E., Antonioli, A., & Boschi, E. (2009). Finite fault inversion of DInSAR coseismic displacement of the 2009 L'Aquila earthquake (central Italy). *Geophysical Research Letters*, *36*(15). https://doi.org/https://doi.org/10.1029/2009GL039293

Atzori, S., & Antonioli, A. (2011). Optimal fault resolution in geodetic inversion of coseismic data. *Geophysical Journal International*, *185*(1), 529–538. https://doi.org/10.1111/j.1365-246X.2011.04955.x.

Atzori, S., Antonioli, A., Tolomei, C., De Novellis, V., De Luca, C., & Monterroso, F. (2019). InSAR full-resolution analysis of the 2017–2018 M>6 earthquakes in Mexico. *Remote Sensing of Environment*, *234*, 111461. https://doi.org/https://doi.org/10.1016/j.rse.2019.111461.

Bechor, N. B. D., & Zebker, H. A. (2006). Measuring two-dimensional movements using a single InSAR pair. *Geophysical Research Letters*, *33*(16). https://doi.org/https://doi.org/10.1029/2006GL026883.

Bradley, K., & Hubbard, J. A. (2025). Updates on the M7.7 Myanmar earthquake. *Earthquake Insights*. https://doi.org/10.62481/9e49eb4a.

Casu, F., Manconi, A., Pepe, A., Manzo, M., & Lanari, R. (2010). Advances in the generation of deformation time series from SAR data sequences in areas affected by large dynamics. *2010 IEEE International Geoscience and Remote Sensing Symposium*, 2618–2621. https://doi.org/10.1109/IGARSS.2010.5651926.

Casu, F., Manconi, A., Pepe, A., & Lanari, R. (2011). Deformation Time-Series Generation in Areas Characterized by Large Displacement Dynamics: The SAR Amplitude Pixel-Offset SBAS Technique. *IEEE Transactions on Geoscience and Remote Sensing*, *49*(7), 2752–2763. https://doi.org/10.1109/TGRS.2010.2104325.

Gray, A. L., Mattar, K. E., Vachon, P. W., Bindschadler, R., Jezek, K. C., Forster, R., & Crawford, J. P. (1998). InSAR results from the RADARSAT Antarctic Mapping Mission data: estimation of glacier motion using a simple registration procedure. *IGARSS '98. Sensing and Managing the Environment. 1998 IEEE International Geoscience and Remote Sensing. Symposium Proceedings. (Cat. No.98CH36174)*, *3*, 1638–1640 vol.3. https://doi.org/10.1109/IGARSS.1998.691662.

Harris, R. A. (1998). Introduction to Special Section: Stress Triggers, Stress Shadows, and Implications for Seismic Hazard. *Journal of Geophysical Research: Solid Earth*, *103*(B10), 24347–24358. https://doi.org/https://doi.org/10.1029/98JB01576.

Hurukawa, N., & Maung Maung, P. (2011). Two seismic gaps on the Sagaing Fault, Myanmar, derived from relocation of historical earthquakes since 1918. *Geophysical Research Letters*, *38*(1). https://doi.org/https://doi.org/10.1029/2010GL046099.

Jiang, H., Feng, G., Wang, T., & Bürgmann, R. (2017). Toward full exploitation of coherent and incoherent information in Sentinel-1 TOPS data for retrieving surface displacement: Application to the 2016 Kumamoto (Japan) earthquake. *Geophysical Research Letters*, 44(4), 1758–1767. https://doi.org/10.1002/2016gl072253.

Massonnet, D., Rossi, M., Carmona, C., Adragna, F., Peltzer, G., Feigl, K., & Rabaute, T. (1993). The displacement field of the Landers earthquake mapped by radar interferometry. *Nature*, *364*(6433), 138–142. https://doi.org/10.1038/364138a0.

Massonnet, D., & Feigl, K. L. (1998). Radar interferometry and its application to changes in the Earth's surface. *Reviews of Geophysics*, *36*(4), 441–500. https://doi.org/https://doi.org/10.1029/97RG03139.

Melgar, D., Weldon, R., Wang, Y., Bato, M. G., Aung, L. T., Shi, X., Wiwegwing, W., Khaing, S. N., Min, S., Thant, M., Speed, C., Zinke, R., Fielding, E., Meltzner, A., & Dawson, T. (2025). Supershear source model of the 2025 M7.8 Myanmar earthquake and paleoseismology of the Sagaing Fault: regions of significant overlap with past earthquakes. Seismica, 4(2). https://doi.org/10.26443/seismica.v4i2.1771.

Mitchell, A., Chung, S.-L., Oo, T., Lin, T.-H., & Hung, C.-H. (2012). Zircon U–Pb ages in Myanmar: Magmatic–metamorphic events and the closure of a neo-Tethys ocean? *Journal of Asian Earth Sciences*, *56*, 1–23. https://doi.org/https://doi.org/10.1016/j.jseaes.2012.04.019.

Okada, Y. (1985). Surface deformation due to shear and tensile faults in a half-space. *Bulletin of the Seismological Society of America*, *75*(4), 1135–1154. https://doi.org/10.1785/BSSA0750041135.

Petersen, G. M., Büyükakpinar, P., Vera Sanhueza, F. O., Metz, M., Cesca, S., Akbayram, K., Saul, J., & Dahm, T. (2023). The 2023 Southeast Türkiye Seismic Sequence: Rupture of a Complex Fault Network. *The Seismic Record*, 3(2), 134–143. https://doi.org/10.1785/0320230008.

Shahzada, K., Noor, U. A., & Xu, Z.-D. (2025). In the wake of the March 28, 2025 Myanmar earthquake: A detailed examination. *Journal of Dynamic Disasters*, *1*(2), 100017. https://doi.org/https://doi.org/10.1016/j.jdd.2025.100017.

Simpson, R. W., & Reasemberg, P. A. (1994). Earthquake-induced static stress changes on central California faults. *U. S. Geol. Surv. Profess Pap. 1550-F*, *F55–F89*.

Socquet, A., Vigny, C., Chamot-Rooke, N., Simons, W., Rangin, C., & Ambrosius, B. (2006). India and Sunda plates motion and deformation along their boundary in Myanmar determined by GPS. *Journal of Geophysical Research: Solid Earth*, *111*(B5). https://doi.org/https://doi.org/10.1029/2005JB003877.

Stein, R. S., King, G. C. P., & Lin, J. (1992). Change in Failure Stress on the Southern San Andreas Fault System Caused by the 1992 Magnitude = 7.4 Landers Earthquake. *Science*, *258*(5086), 1328–1332. https://doi.org/10.1126/science.258.5086.1328.

Tha Zin Htet Tin, Nishimura, T., Hashimoto, M., Lindsey, E. O., Aung, L. T., Min, S. M., & Thant, M. (2022). Present-day crustal deformation and slip rate along the southern Sagaing fault in Myanmar by GNSS observation. *Journal of Asian Earth Sciences*, *228*, 105125. https://doi.org/https://doi.org/10.1016/j.jseaes.2022.105125.

USGS (2025). *M 7.7 - 2025 Mandalay, Burma (Myanmar) Earthquake*. https://earthquake.usgs.gov/earthquakes/eventpage/us7000pn9s/executive.

Vera, F., Carrillo-Ponce, A., Crosetto, S., Kosari, E., Metzger, S., Motagh, M., Liang, Y., Lyu, S., Petersen, G., Saul, J., Sudhaus, H., Symmes-Lopetegui, B., Than, O., Xiao, H., & Tilmann, F. (2025). *Supershear Rupture Along the Sagaing Fault Superhighway: The 2025 Myanmar Earthquake*. https://doi.org/10.22541/essoar.175034871.19414276/v1.

Vigny, C., Socquet, A., Rangin, C., Chamot-Rooke, N., Pubellier, M., Bouin, M.-N., Bertrand, G., & Becker, M. (2003). Present-day crustal deformation around Sagaing fault, Myanmar. *Journal of Geophysical Research: Solid Earth*, *108*(B11). https://doi.org/https://doi.org/10.1029/2002JB001999.

Walker, K. T., & Shearer, P. M. (2009). Illuminating the near-sonic rupture velocities of the intracontinental Kokoxili Mw 7.8 and Denali fault Mw 7.9 strike-slip earthquakes with global P wave back projection imaging. *Journal of Geophysical Research: Solid Earth*, *114*(B2). https://doi.org/https://doi.org/10.1029/2008JB005738.

Wang, Y., Sieh, K., Tun, S. T., Lai, K.-Y., & Myint, T. (2014). Active tectonics and earthquake potential of the Myanmar region. *Journal of Geophysical Research: Solid Earth*, *119*(4), 3767–3822. https://doi.org/https://doi.org/10.1002/2013JB010762.

Williams, C. A., & Wadge, G. (1998). The effects of topography on magma chamber deformation models: Application to Mt. Etna and radar interferometry. *Geophysical Research Letters*, *25*(10), 1549–1552. https://doi.org/https://doi.org/10.1029/98GL01136.

Zelenin, E., Bachmanov, D., Garipova, S., Trifonov, V., & Kozhurin, A. (2022). The Active Faults of Eurasia Database (AFEAD): the ontology and design behind the continental-scale dataset. *Earth System Science Data*, *14*(10), 4489–4503. https://doi.org/10.5194/essd-14-4489-2022.

Zeng, H., Ma, Z., Li, C., Yin, X., Jiang, Y., Chen, Y., Rosakis, A., Konca, O., & Wei, S. (2025). Super-Shear and Generalized Rayleigh Rupture of the 2023 Turkey Earthquake Doublet Influenced by Fault Material Contrast. *Journal of Geophysical Research: Solid Earth*, 130(6). https://doi.org/10.1029/2025jb031560.

Corresponding author: valerio.ruocco@studentmail.unicas.it